Solid Freeform Fabrication 2024: Proceedings of the 35th Annual International Solid Freeform Fabrication Symposium – An Additive Manufacturing Conference
Reviewed Paper

Initial Layer Characterization for Multilayer Fluid Interface Supported Printing

Brody Oliver, Stacy Ross, Yongxin Wu, Amit Jariwala*

Georgia Institute of Technology
George W. Woodruff School of Mechanical Engineering

*amit.jariwala@gatech.edu

Abstract

A new additive manufacturing technique for Stereolithography (SLA) that reduces the need for sacrificial supports is in development. Traditional SLA requires sacrificial supports for overhanging geometry, which consume excess material, require post-processing, and reduce surface quality. To reduce the need for supports, fluid interface supported printing (FISP) cures from a thin resin layer above an inert, immiscible supporting fluid. Density differences between the support fluid and resin are intended to prevent deflection. Current research aims to improve print quality and minimize print deformation through experimentation and multiphysics simulation. With the current system, the relationship between cure depth and energy input has been quantified, and multilayer prints were proven feasible. Significant warpage has occurred in unsupported overhanging layers. This motivated experimentation incorporating surfactants to encourage even resin spreading, and incorporating grayscaling to reduce curling due to rapid polymerization. Although resin spreading remains an issue, qualitative observation shows grayscaling reduced layer curling.

Glossary

AM: Additive Manufacturing

BAPO: phenylbis (2,4,6-trimethylbenzoyl)-phosphine oxide

DLP: Digital Light Processing

FISP: Fluid Interface Supported Printing

IPA: Isopropyl Alcohol

SLA: Stereolithography

TPO: diphenyl (2,4,6-trimethylbenzoyl) phosphine oxide

UV: Ultraviolet

1. Introduction

Stereolithography (SLA) is a desirable form of additive manufacturing due to its high resolution, though the need for sacrificial support structures limits its capabilities. A traditional SLA setup includes a resin vat, light source, and build plate. Resin refers to a mixture of monomers and photoinitators. The light source provides activation energy to the photoinitators and consequently photopolymerization occurs. Through photopolymerization, the liquid resin is transformed into a cross-linked polymer [1]. The light source is manipulated into the desired shape, referred to as a mask. After the initial layer is cured upon the build plate, it is moved away from the curing surface and the process is repeated to create each subsequent layer. Because SLA utilizes light to create solid structures, it offers higher precision than extrusion based additive manufacturing. In extrusion-based printing, the print resolution is limited by the nozzle size. Conversely, the resolution of SLA is defined by photons, allowing a layer thickness as small as 1μm [2]. A primary limitation of traditional stereolithography is the need for support structures while printing overhanging features.

Fluid Interface Supported Printing (FISP) seeks to expand the capabilities of stereolithography printing by minimizing or eliminating the need for sacrificial support structures. Traditional stereolithography creates high resolution structures through photopolymerization but requires sacrificial support structures for overhanging geometry. Sacrificial supports consume excess time and materials, and their removal results in a lower surface quality. By curing a thin layer of resin atop an inert, immiscible support fluid, buoyant forces can counteract sagging of overhanging geometry, which would traditionally require extraneous support structures. The complex chemical reactions and fluid dynamics of the system pose a challenge in creating robust controls and consistent print quality. Experimental deformation reduction and a multiphysics COMSOL model are employed in parallel to increase feasibility for this process. Ensuring prints form without significant curling or warpage is a primary challenge this research seeks to solve. The objective of this research is to further the development of Fluid Interface Supported Printing (FISP), which has potential to improve and broaden the applications of stereolithography.

2. Setup

2.1. Experimental Setup

Currently, the FISP system uses a Wintek PRO4710 digital light processing (DLP) 405nm UV light projector to project digital masks upon the curing platform. The projection passes through a 0.5OD neutral density filter to achieve the desired light intensity before hitting the cure surface. The cure surface is a thin layer of Anycubic Clear resin atop the support fluid. AnyCubic resin has been selected for its consistent chemical characteristics and relatively low viscosity, which allows the resin to spread quickly. The fluid interface supported printing mimics a traditional top-down stereolithography system but incorporates support fluid to support overhanging geometry during printing. The support fluid is a saline solution with density equal

to the density of cured resin to counteract the force of gravity, comprised of 24.7% non-iodized salt and 75.3% deionized water (by weight).

The print bed is a cantilever stainless steel plate which is moved vertically using an ASI MS2000 motorized staging control. Initially, the print bed is zeroed at the curing surface. Gradually, as layers are cured, the print bed is lowered into the vat of support fluid, creating the desired geometry using a top-down manufacturing method. Resin is replenished throughout the print and support fluid is removed to maintain the height of the cure region.

Maintaining the cure height is important to ensure consistent light intensity throughout the print. The system, shown in Figure 1, incorporates stage adjustment to allow precise alignment of the curing region. Because the resin is being replenished during printing, it must spread quickly to create a uniform layer.

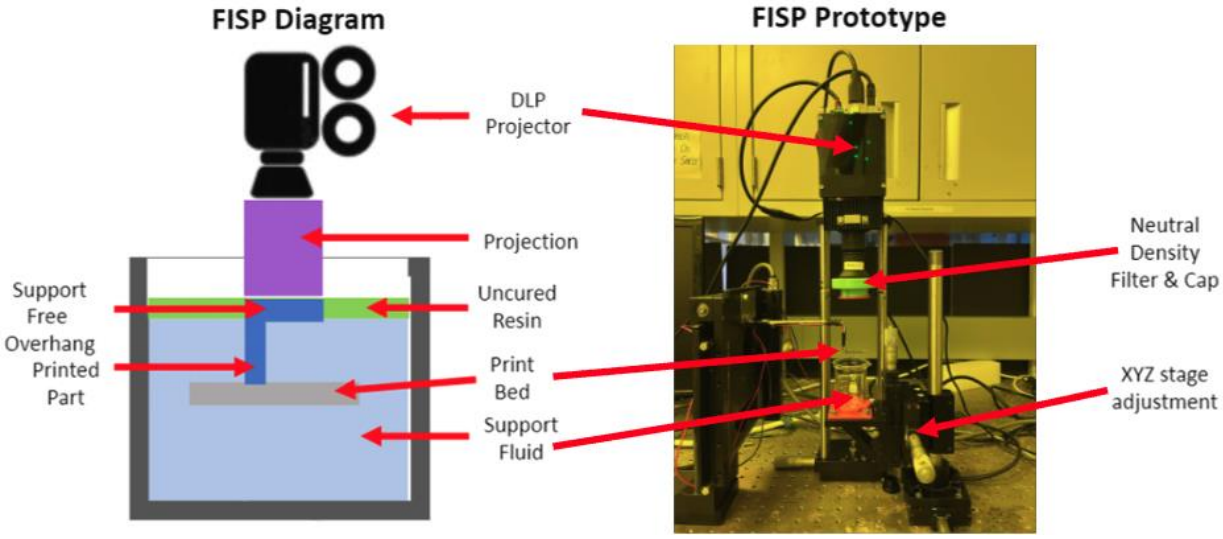

Figure 1: Fluid Interface Supported Printer Setup.

2.2. Post Processing Setup

Although post processing is minimized by excluding sacrificial supports, the resulting prints of the FISP system still require rinsing and flood curing. The AnyCubic wash and cure station, shown in figure 2, is used to complete post-processing for each test sample.

Figure 2: AnyCubic Wash and Cure Station [3].

The samples undergo a rinse cycle of 1 minute using 99% isopropyl alcohol (IPA) to remove uncured resin.

Finally, the samples are flood cured using the AnyCubic light source for 30s to completely cure any partially cured resin. Ensuring the samples are completely cured reduces the likelihood of inaccurate measurements due to deformation caused by the measurement device and ensures consistency across samples.

3. Cure Depth Characterization

3.1. Experimental Method

Experiments of resin cure depth against light exposure time have been conducted to characterize the resin curing process using the new DLP setup. 20mL of resin is transferred to a souffle cup, which is placed under the DLP projector. The distance from the projector lens to the top of the resin surface is adjusted to be 114mm, to ensure optimal projection focus for the 114mm projector. The projector then projects a circular image, as shown in Figure 4, onto the resin for a set projection time, before the souffle cup is removed and the cured shape is washed and cured. After washing and post-curing, the cured shape is measured with a micrometer at 3 locations in the center, and the average of the measurements is taken as the cure depth. A flow chart outlining the steps of this experiment is shown in figure 3.

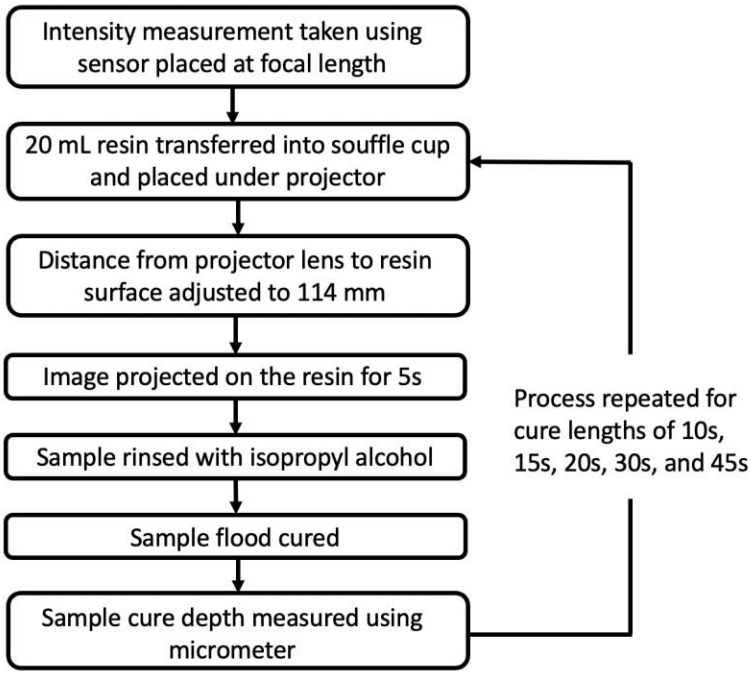

Figure 3: Cure Depth Characterization Experiment Flowchart.

3.2. Results

Initial cure tests at projection times of 10s and longer resulted in deformation of the cured layer into 2 parts, usually in a triangular pattern. To cure the edges first and prevent curling from the sides, the projected image was modified to be a circle which is darker in the center, as shown in figure 4. The gray scaled image was observed to reduce curling around the edges and produce a print with a more uniformly circular shape when compared to a projected circle of uniform intensity.

The light intensity was measured to be 1.1mW/cm2 at the gray center portions of the projection, when the DLP projector was set to 9500mA current for all 3 LEDs (RGB). Thickness measurements were taken from the central area of the print, the region cured by the darker circle of the projected image to avoid the potentially thicker edge of the print.

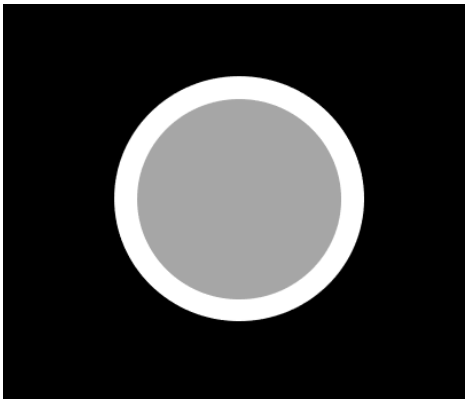

Figure 4: Projected gray scale image to reduce deformation.

The following results shown in figure 5 were obtained for exposure times from 5 to 45s.

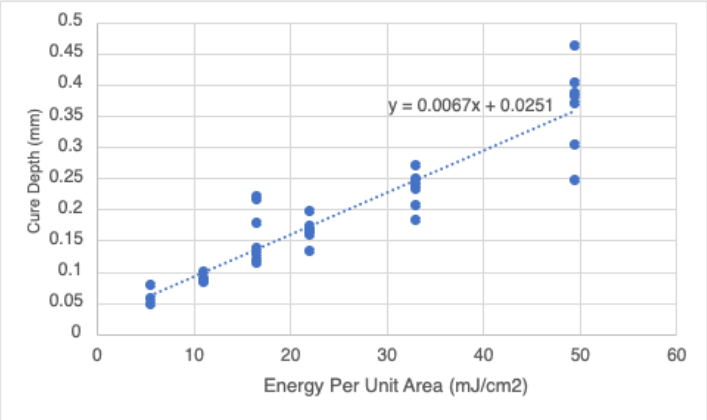

Figure 5: Plot of Cure Depth (mm) against Energy Per Unit Area (mJ/cm2).

Cure depth was observed to generally increase with energy per unit area as expected. However, due to increased unevenness in warping, readings taken at higher exposure times have greater variance.

4. Simulation

A multiphysics model has been implemented to predict cure depth of FISP and determine whether the observed curing behavior is consistent. The reaction kinetics of the polymerization in the fluid interface supported printer are simulated using COMSOL. Boundary conditions are set to reflect the resin interfacing with the open air above and the support fluid below. Oxygen dissolved in air and the support fluid slows down the polymerization process within the resin through a process called oxygen inhibition. Understanding the interaction of these three fluids is vital in correctly predicting the behavior of the system. In the simulation, the light source provides 3.0 mW/cm^2 intensity to the curing surface. As cure time increases, the energy absorbed by the resin increases, more free radicals are generated, and increased polymerization occurs. As shown in figure 6, the simulation produces a plot of degree polymerization for the cure profile. Table 1 contains the model parameters used for the resin in the simulation [4].

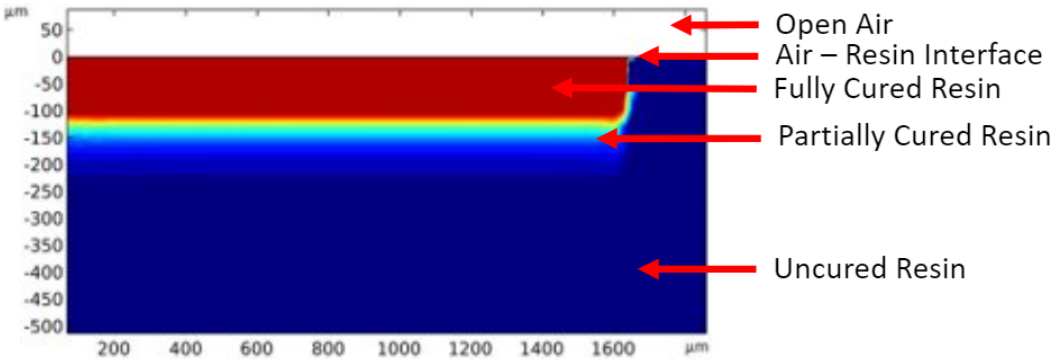

Figure 6: COMSOL Simulation of 5s Cure Profile.

Table 1: Current model parameters

Parameter	Variable Name	Units	Emami	Current
Initial concentration of O2 in resin	c_O2_0	mol/m^3	1.05	0.9
Quantum yield	Phi	-	0.6	0.6
Molar absorptivity	ep0	m^2/mol	14	75
Molecular weight of monomers	MW_monomer	kg/mol	0.296	0.27836
Molecular weight of initiator	MW	kg/mol	0.256	0.3404
Weight % of photoinitiator	wt	-	2	10
Density of monomers	Density_Monomer	kg/m^3	1110	953.67
Oxygen diffusion rate	DO2	m^2/s	1e-10	1e-10

Values are taken from Emami and Rosen's updated model [5], with some data provided by Anycubic [6]. Multiple deviations from the values given Emami and Rosen's paper have been made to more accurately reflect the experimental set up. The initial concentration of CO2 in the resin was changed from Emami and Rosen's value of 1.05 to the value in the current model of 0.9 to account for the findings of a publication on oxygen solubility in diacrylates [7]. The molar absorptivity parameter was increased from 14 to 75 because the photoinitiator in the resin currently used is phenylbis (2,4,6-trimethylbenzoyl)-phosphine oxide (BAPO) as opposed to diphenyl (2,4,6-trimethylbenzoyl) phosphine oxide (TPO). The value of 75 was drawn from Dietlin's 2019 paper [8]. Molecular weight and density were derived from specifications provided by the resin manufacturer [6].The weight percentage of photoinitiator is effectively 10% for the Anycubic resin compared to active monomers. The model uses an "Extremely fine" mesh size corresponding to mesh elements with a height of 12 um. Excessive polymerization results in poor layer adhesion while inadequate polymerization leaves the layer unfinished. Therefore, predicting the depth of cure for a given time is an important step in developing a high quality, repeatable FISP appropriate for multilayer curing.

Currently, the experimental results and the results of the simulation do not agree, prompting further investigation into and experimentation with methods to reduce warping and inconsistency in print layer height.

5. Multi-Layer Cures

5.1. Experimental Method

Multi-layer cures were attempted with the new setup to validate the merits of FISP and explore challenges to further realization of the FISP system. Multilayer cantilevers and bridges were attempted using the settings shown in Table 2.

Table 2: Multilayer Print Parameters.

LED Current	Projection Time	Layer Height	Settling Time	Irradiation
9500 mA	4.5s	0.2mm	20s	0.9 mW/cm^2

For the multi-layer cures, the print bed is first zeroed to lie between the resin and support fluid interface. A Python script is used to automatically flash the relevant print images at the set projection time, before controlling the print bed to move down by the layer height and waiting a set amount of time (settling time) to allow the resin to spread evenly over the surface again. First, a base consisting of 10 layers of either one or two squares is flashed, corresponding to the cantilever and bridge cures respectively. After the initial 10 layers, another 10 layers of overhang geometry, in this case, a rectangle extending over and past the square base layers, is flashed to create either the bridge or cantilever. 10uL of resin is added after the base layer curing is complete but prior to the curing of the overhang. A flow chart outlining the steps of this experiment is shown in figure 7.

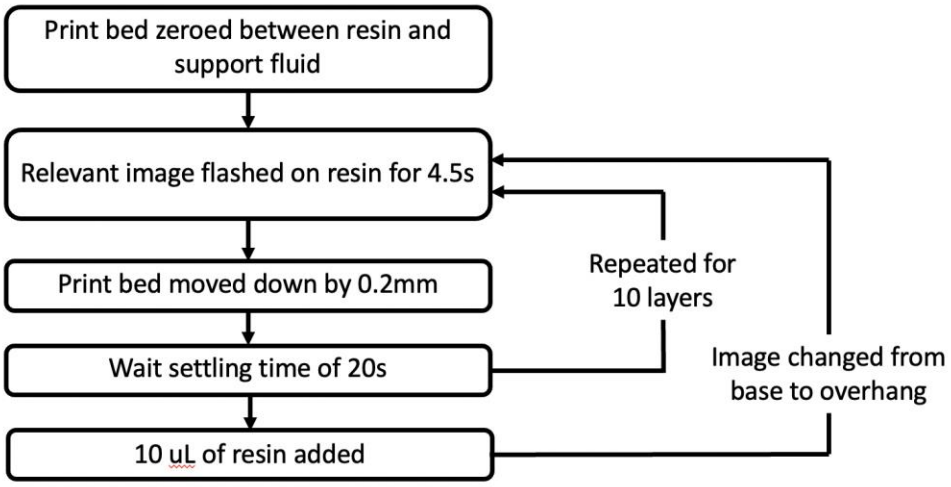

Figure 7: Cure Depth Characterization Experiment Flowchart.

5.2. Results

The main issue faced when attempting both types of cures was warping on the layer surface. An acceptable base was always formed, however the curing of unsupported overhangs resulted in warping that causes the overhanging portion to curl upwards and stick out above the resin layer. This caused subsequent layers to fail to cure over the overhanging portion.

Another issue was delamination between layers, especially between the square base and overhang layers. This could be due to the greater warping forces on the larger overhang layer peeling it away before it can fully cure to the existing layers. Subsequent flood curing of the

multi-layer cure resulted in proper adhesion between layers, even those which had delaminated, indicating incomplete curing at the tested settings.

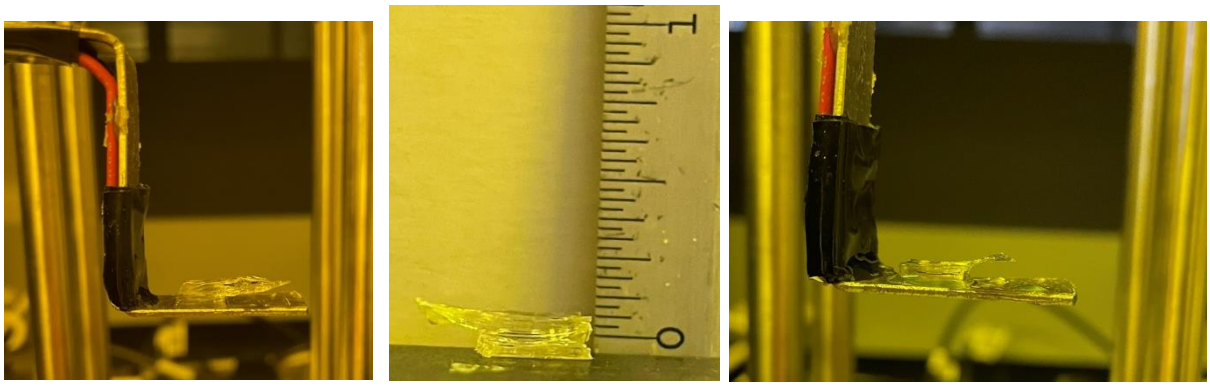

Figure 8: Attempted multi-layer cantilever cures.

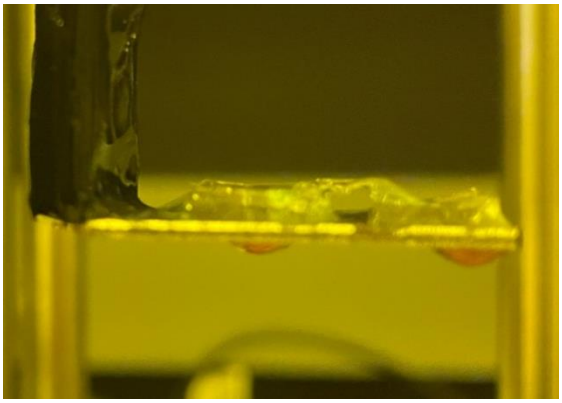

Figure 9: Attempted multi-layer bridge cure.

6. Surfactant Layer

6.1. Background

One persistent issue observed during the cure depth experiments, especially at longer cure intensities with higher warping, was unevenness in the resin layer when it was deposited on the support fluid. The non-polar resin does not spread well over the polar saline support fluid, and as such does not form an even layer. This results in uneven layer thicknesses when cured, as well as inconsistent warping between samples.

To address this issue, it was theorized that a surfactant layer in between the resin and support fluid could help enhance resin spreading. Surfactants have both a polar head and a non-

polar tail. When deposited on the support fluid, it can form a Langmuir layer where the surfactants reorientate to have their nonpolar tails face away from the support fluid. This provides a non-polar surface upon which the resin could theoretically spread more evenly.

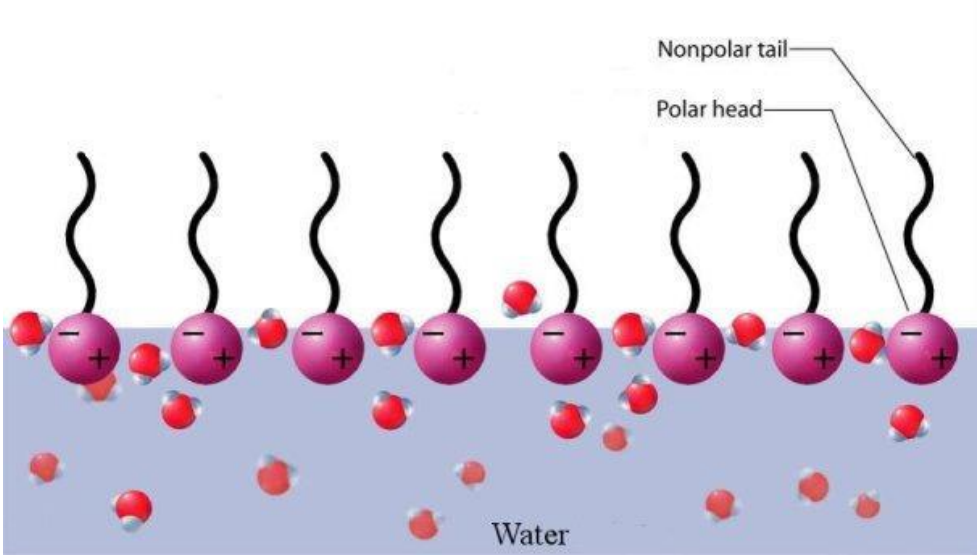

Figure 10: Illustration of Langmuir Layers [9].

6.2. Experimental Method

4mg of stearic acid (Sigma-Aldrich Product No. 175366-100G, 95% reagent grade) was well mixed with 40mL of hexane (Sigma-Aldrich Product No. 208752-500ML, 95% reagent grade). A set volume of this solution was then pipetted onto the dyed support fluid surface, and the hexane was allowed to fully evaporate. The surfactant layer was then observed, before 20uL of resin was deposited onto the resin to be observed. 20uL, 40uL, 160uL and 200uL volumes of surfactants were deposited using a 20uL micropipette.

6.3. Result

Both 20uL and 40uL resulted in a small island of surfactant leftover that resin cannot spread over, while the 160uL and 200uL tests resulted in the entire support fluid surface being covered in surfactant. This surfactant covered surface impeded resin spreading rather than improve it, likely due to the surface tension required to displace the surfactant.

The surfactant layers were actively detrimental to resin spreading, as the islands of surfactants left behind at higher amounts prevented resin from spreading into the surfactant areas. This results in patches above the support fluid without resin. Even at lower surfactant amounts, the evaporation of the hexane proceeds from outside in, which pulls and concentrates the surfactants into a small island which also impedes resin spreading.

While other surfactants, solvents, and concentrations may produce the desired result of promoting resin spreading, it was concluded based on experimental results the stearic acid and hexane solution used was unsuitable for this purpose.

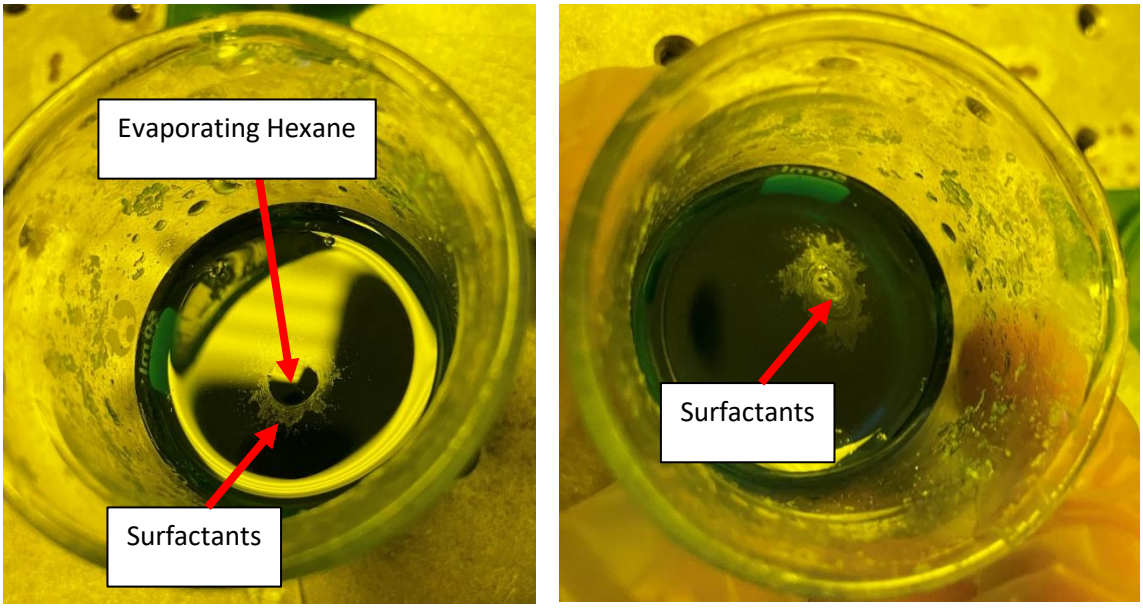

Figure 11: 20uL surfactant deposition.

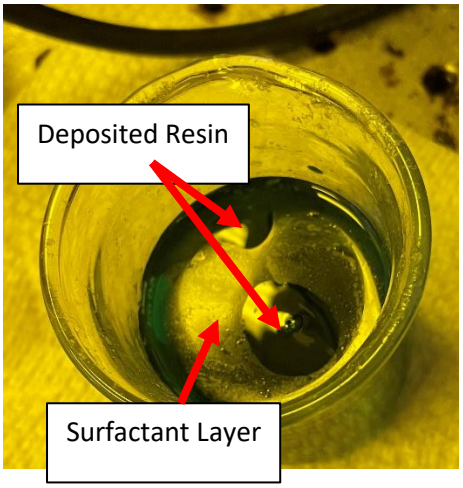

Figure 12: 200uL surfactant deposition.

7. Future Work

As observed when attempting multi-layer cures, the main challenge that needs to be resolved to realize successful multi-layer FISP prints is to reduce or eliminate warping in the topmost layer, especially for overhang layers. There are several potential avenues that can be explored to potentially solve this issue.

The use of a surfactant layer could be explored further with different surfactants, solvents, and concentrations. In addition, more quantifiable methods can be used to evaluate the impact of the surfactant. One method is the use of an interferometric setup to measure the amount of time it takes for the resin to stop spreading and settle on the support surface [10]. Another method is to use a contact angle setup to quantify the contact angle formed between the surfactant and resin at various times. Once the warping issues are resolved, the full system can be designed.

To make the system suitable for proper multi-layer 3D prints, an automated system for refilling resin would be required. A challenge this system will face is in accurately dispensing the desired volumes of resin. The small volume of resin consumed with each layer, coupled with the viscous nature of the resin, could make accurate dispending challenging. The system must also be able to pause printing while the dispensed resin spreads and settles evenly over the support fluid.

A system to control the support fluid height may also be required, as the cured resin will displace support fluid when lowered into it, raising the support fluid and resin layer. This may result in the resin layer misaligning with the top surface of the current print, as well as the resin layer distance to the projector decreasing to below the recommended 114mm distance. Some form of pump or reservoir head can be implemented to remove support fluid and maintain the resin layer height [11].

Using a vat with a relatively large surface area and volume compared to the print can help alleviate these issues, as the resin layer volume, and hence height, should change negligibly with each layer cured, allowing less precision in resin refill and controlling support fluid height.

8. Conclusions

Cure depth characterization experiments demonstrate inconsistencies due to warping and delamination but follow an expected trend. To aid in future developments, flux conditions and improved reaction kinematics were incorporated into a cure profile simulation. Initial multi-layer cures with unsupported overhangs were also produced on the FISP system, albeit with notable warping at the overhang layer. This caused delamination of the overhang layer, as well as prevented further layers from being cured on top of the warped overhang areas. Unevenness in the spreading resin layer was observed to cause inconsistent layer thickness and warping. Stearic acid surfactant was tested to encourage even resin spreading but tended to clump into islands, which actively hindered resin spreading. Stearic acid surfactant was determined not to be a viable solution to consistency and warping issues. Areas for future work towards a fully realized FISP system is proposed, primarily focused on minimizing warping, improving consistency, as well as other required components in a full FISP system.

9. Acknowledgements

The authors would like to thank Dr. Robert Schwerzel for advising this research. Thank you to other members of the research team, Siva Appana and Christian Sims, for volunteering their time and effort. Thank you to Flowers Invention Studio for fabrication assistance. Thank you to the George W. Woodruff School of Mechanical Engineering for supporting this research.

References

[1] S. Zakeri, M. Vippola and E. Levanen, "A Comprehensive Review of the Photopolymerization of Ceramic Resins Used in Stereolithography," *Additive Manufacturing,* vol. 35, no. 2214-8604, 2020.

[2] P. Lakkala, S. R. Munnangi, S. Bandari and M. Repka, "Additive Manufacturing Technologies with Emphasis on Stereolithography 3D Printing in Pharmaceutical and Medical Applications: A review," *International Journal of Pharmaceutics,* vol. 5, no. 100159, 2023.

[3] AnyCubic, "Anycubic Wash & Cure 3," [Online]. Available: https://store.anycubic.com/products/wash-cure-3?variant=43680321798306. [Accessed April 2024].

[4] S. Ross, C. Sims, S. Appana, R. Schwerzel and J. S. Amit, "Process Modeling For Fluid-Interface Supported Resin Printing," in *Proceedings of the 34th Annual International Solid Freeform Fabrciation Symposium - An Additive Manufacturing Conference,* Austin, TX, 2023.

[5] M. M. Emami and D. W. Rosen, "An Improved Vat Polymerization Cure Model Demonstrates Photobleaching Effects," in *Proceedings of the 29th Annual International Solid Freeform Fabrication Symposium - An Additive Manufacturing Conference,* Austin, TX, 2018.

[6] Shenzhen AnyCubic Technology Co., "UV Resin: SDS Report," Standards Technical Services, 2019.

[7] T. Scherzer and H. Langguth, "Temperature Dependence of the Oxygen Solubility in Acrylates and its Effect on the Induction Period in UV Photopolymerization," *Macromolecular Chemistry and Physics,* vol. 206, pp. 240-245, 2005.

[8] C. Dietlin, "Rational Design of Acyldiphenylphosphine Oxides as Photoinitiators of Radical Polymerization," *Macromolecules,* 2019.

[9] "Langmuir-Blodgett Film," Wikipedia, 27 April 2024. [Online]. Available: https://en.wikipedia.org/wiki/Langmuir%E2%80%93Blodgett_film. [Accessed 1 May 2024].

[10] X. Zhao and D. W. Rosen, "Real-time Interferometric Monitoring and Measuing of Photopolymerization Based Stereolithography Additive Manufacturing Process: Sensor Model Algorithm," *Measurmeent Science and Technology,* vol. 28, 2016.

[11] C. W. Beh, D. S. Yew, r. J. Chai, S. Y. Chin, Y. Seow and S. S. Hoon, "A Fluid-Supported 3D Hydrogel Bioprinting Method," *Biomaterials,* vol. 276, 2021.

[12] S. C. Ligon, B. Husar, H. Wutzel, R. Holman and R. Liska, "Strategies to Reduce Oxygen Inhibition in Photoinduced Polymerization," *American Chemical Society,* vol. 114, pp. 557-589, 2013.

[13] N. Mulka, T. Goyal, A. Jariwala and D. Rosen, "Statics Liquid Interface To Reduce Support Structure Necessity in Top-Down Stereolithography," in *Solid Freeform Fabrication 2021: Proceedings of the 32nd Annual International Solid Freeform Fabrication Symposium - An Additive Manufacturing Conference*, Austin, TX, 2021.

[14] J. R. Tumbleston, D. Shirvanyants, N. Ermoshkin, R. Janusziewicz, A. R. Johnson, D. Kelly, K. Chen, R. Pinschmidt, J. P. Rolland, A. Ermoshkin, E. T. Samulski and J. M. Desimone, "Continous Liquid Interface Production of 3D Objects," *Science,* vol. 347, no. 6228, pp. 1349-1352, 2015.

[15] K. Gao, B. L. Ingenhut, A. Van de Ven, F. V. Mackenzie and A. Cate, "Multiphysics Modeling of Photo-Polymerization in Stereolithography Printing Process and Validation," 2018. [Online]. Available: https://www.comsol.com/paper/multiphysics-modeling-of-photo-polymerization-in-stereolithography-printing-proc-66011. [Accessed May 2024].

[16] A. Khadilkar, J. Wang and R. Rai, "Deep Learning-based Stress Prediction for Bottom-Up SLA 3D Printing Process," *The internation Journal of Advanced Manufacturing Technology,* vol. 102, pp. 2555-2569, 2019.